

# Low-Temperature Self-Limiting Growth of III-Nitride Thin Films by Plasma-Enhanced Atomic Layer Deposition

Necmi Biyikli\*, Cagla Ozgit, and Inci Donmez

*UNAM–Institute of Materials Science and Nanotechnology, Bilkent University, Ankara 06800, Turkey*

We report on the low-temperature self-limiting growth and characterization of III-Nitride thin films. AlN and GaN films were deposited by plasma-enhanced atomic layer deposition (PEALD) on various substrates using trimethylaluminum (TMA), trimethylgallium (TMG) and triethylgallium (TEG) as group-III, and ammonia (NH<sub>3</sub>) as nitrogen precursor materials. Self-limiting growth behavior, which is the major characteristic of an ALD process, was achieved for both nitride films at temperatures below 200 °C. AlN deposition rate saturated around 0.86 Å/cycle for TMA and NH<sub>3</sub> doses starting from 0.05 and 40 s, respectively, whereas GaN growth rate saturated at a lower value of 0.56 Å/cycle and 0.48 Å/cycle for TMG and TEG doses 0.015 s and 1 s, respectively. The saturation dose for NH<sub>3</sub> was measured as 90 s and 120 s, for TMG and TEG experiments, respectively. Within the self-limiting growth temperature range (ALD window), film thicknesses increased linearly with the number of deposition cycles. At higher temperatures ( $\geq 225$  °C and  $\geq 350$  °C for AlN and GaN respectively), deposition rate became temperature-dependent, with increasing growth rates. Chemical composition and bonding states of the films deposited within the self-limiting growth regime were investigated by X-ray photoelectron spectroscopy (XPS). GaN films exhibited high oxygen concentrations regardless of the precursors choice, either TMG or TEG, whereas low-oxygen incorporation in AlN films was confirmed by high resolution Al 2p and N 1s spectra of AlN films. AlN films were polycrystalline with a hexagonal wurtzite structure regardless of the substrate selection as determined by grazing incidence X-ray diffraction (GIXRD). GaN films showed amorphous-like XRD signature, confirming the highly defective layers. High-resolution transmission electron microscopy (HR-TEM) images of the AlN thin films revealed a microstructure consisting of several-nanometer sized crystallites, whereas GaN films exhibited sub-nm small crystallites dispersed in an amorphous matrix.

**Keywords:** III-Nitride, AlN, GaN, Thin Film, Atomic Layer Deposition, Low-Temperature, Self-Limiting Growth, Structural Characterization.

## 1. INTRODUCTION

III-Nitride material family (AlGaInN) is known as wide bandgap semiconductors. Owing to their wide and direct bandgap ranging from 3.4 to 6.2 eV, AlN, GaN, and their ternary alloys Al<sub>x</sub>Ga<sub>1-x</sub>N, offer unique combination of material properties for a number of critical applications including UV optoelectronics (blue/violet light sources, UV/visible/solar-blind photodetectors), high-power and high-frequency electronics (field-effect transistors, high-electron mobility transistors), photovoltaic solar cell and thin-film-transistor (TFT) insulating layers, chemical gas sensors, surface acoustic wave devices, and piezoelectric transducers.<sup>1–7</sup>

Metal-organic chemical vapor deposition (MOCVD), offers the most efficient growth process for III-Nitride

thin films due to its ability to deposit high quality materials with significant growth rates, however the deposition of Al<sub>x</sub>Ga<sub>1-x</sub>N thin films requires high temperatures, typically above 1000 °C.<sup>8</sup> Deposition of III-Nitride layers on temperature-sensitive device layers and substrates (e.g., CMOS wafers, low-temperature compatible glass and flexible polymeric substrates), requires the development of low-temperature growth methods.

Atomic layer deposition (ALD) is a special type of low-temperature chemical vapor deposition, in which the substrate surface is exposed to sequential pulses of two or more precursors separated by purging periods.<sup>9,10</sup> Unless decomposition of the precursor occurs, each pulse leads to surface reactions that terminate after the adsorption of a single monolayer. When compared to other low-temperature methods, ALD stands out with its self-limiting growth mechanism, which enables the deposition of highly conformal thin films with sub-nanometer thickness control.

\*Author to whom correspondence should be addressed.

There have been a few reports on the growth of  $\text{Al}_x\text{Ga}_{1-x}\text{N}$  thin films using ALD technique. ALD growth of AlN has been studied by several research groups.<sup>11–16</sup> Lee et al.<sup>11</sup> reported plasma-enhanced ALD (PEALD) of AlN at 350 °C using aluminum chloride ( $\text{AlCl}_3$ ) and  $\text{NH}_3/\text{H}_2$  plasma. Growth rate of this process saturated at  $\sim 0.42$  Å/cycle, resulting with films composed of microcrystallites of wurtzite (100) in an amorphous AlN matrix.<sup>12</sup> Thermal,<sup>13,14</sup> plasma-enhanced,<sup>14</sup> and UV-assisted<sup>15</sup> ALD of AlN using TMA and  $\text{NH}_3$  have been studied within the temperature ranges of 320–470, 250–470, and 240–370 °C, respectively—however, no self-limiting growth behavior was observed. This was explained by Riihela et al.<sup>13</sup> by the fact that surface reactions between TMA and  $\text{NH}_3$  occur with reasonable rates only at temperatures where TMA self-decomposition takes place. Recently, Kim et al.<sup>16</sup> have reported remote plasma ALD of amorphous AlN thin films using TMA and  $\text{N}_2/\text{H}_2$  plasma. In their study, growth rate saturated at  $\sim 1.25$  Å/cycle within the range of 100–400 °C and then decreased with increasing temperature. For GaN, only one recent report exists in which Kim et al.<sup>17</sup> deposited GaN thin films by thermal ALD using  $\text{GaCl}_3$  and  $\text{NH}_3$  as the gallium and nitrogen precursors, respectively. They achieved self-limiting growth at a deposition rate of  $\sim 2.0$  Å/cycle within the temperature range of 500–750 °C.

In this report, we summarize our low-temperature self-limiting III-Nitride material growth and structural characterization efforts using PEALD technique. Both AlN and GaN thin films were deposited in the self-limiting growth regime below 200 °C. ALD process parameters including group-III precursor and  $\text{NH}_3$  pulse times,  $\text{NH}_3$  flow rate, purge time, and deposition temperature were investigated in order to achieve self-limiting growth conditions for both AlN and GaN films. Structural characterization results of the films deposited within the ALD window are also presented.

## 2. EXPERIMENTAL DETAILS

Depositions were carried out in a Fiji F200-LL ALD reactor (Cambridge Nanotech Inc.) with a base pressure of  $\sim 0.25$  torr, using Ar as the carrier gas.  $\text{NH}_3$  flow rate and plasma power were kept constant at 50 sccm and 300 W, respectively. System was purged for 10 seconds after each precursor exposure. Prior to depositions, pre-cleaned substrates were dipped into dilute HF solution for  $\sim 1$  min, then rinsed with DI-water and dried with  $\text{N}_2$ .

Film thicknesses were estimated by using variable angle spectroscopic ellipsometry (VASE, J.A. Woollam). Ellipsometric spectra of the samples that were recorded at three angles of incidence ( $65^\circ$ ,  $70^\circ$ ,  $75^\circ$ ) in the wavelength range of 400–1200 nm, were fitted by using the Cauchy dispersion function. An energy dispersive system (Genesis Apex 4, AMETEK) attached to a Nova

NanoSEM (FEI) scanning electron microscope (SEM) was used for elemental analysis. Chemical composition and bonding states of the grown films were determined by a Thermo Scientific K-Alpha spectrometer with a monochromatized Al  $K\alpha$  X-ray source, which was used for the X-ray photoelectron spectroscopy (XPS) studies. Crystallinity of the films was investigated using grazing-incidence X-ray diffraction (GIXRD) measurements which were performed in a PanAnalytical X'Pert PRO MRD diffractometer using Cu  $K\alpha$  radiation. FEI Tecnai G2 F30 transmission electron microscope was used for the imaging of samples prepared by FEI Nova 600i Nanolab focused ion beam (FIB) system.

## 3. RESULTS

### 3.1. PEALD of AlN

Figure 1(a) shows the saturation curves of aluminum and nitrogen precursors at 185 °C. For the TMA saturation

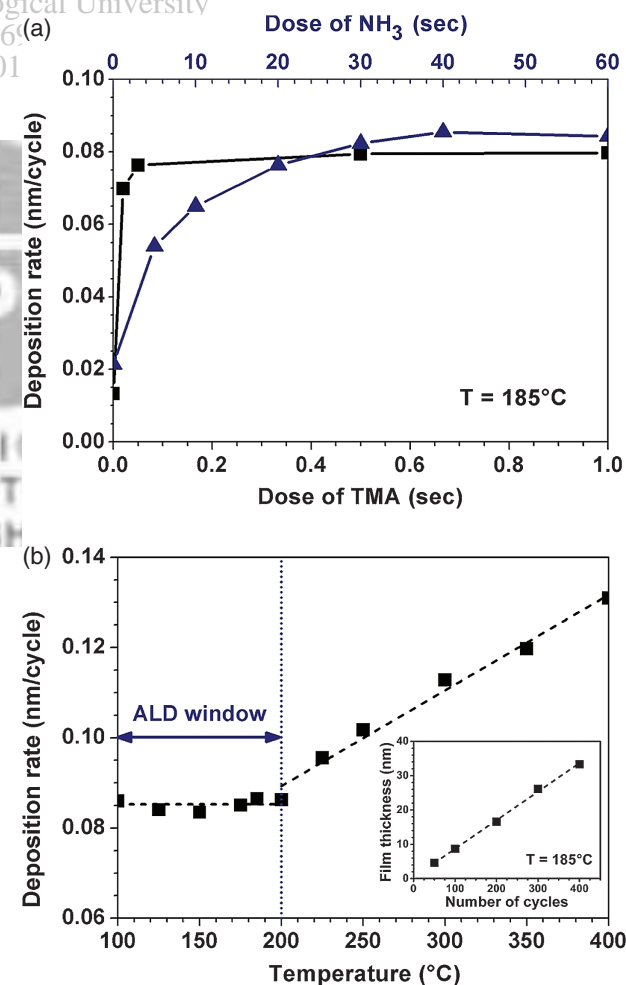


**Fig. 1.** (a) Precursor saturation curves for AlN films:  $\text{NH}_3$  dose was kept constant at 20 seconds for the TMA saturation curve (■), and TMA dose was kept constant at 0.05 seconds for the  $\text{NH}_3$  saturation curve (▲). (b) Deposition rates of AlN thin films at different temperatures. (Inset) Film thickness versus number of deposition cycles.

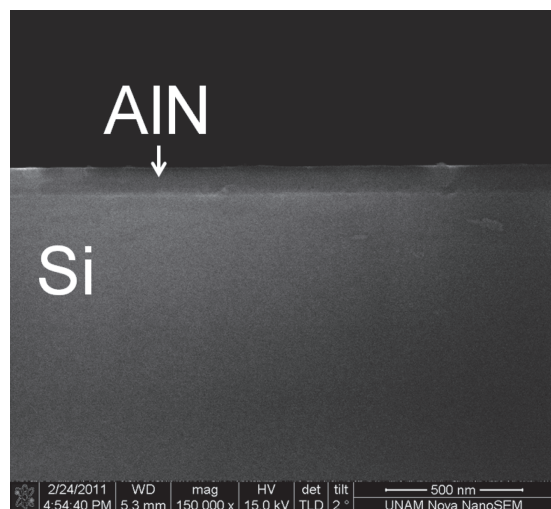


Fig. 2. Cross-sectional SEM image of the  $\sim 100$  nm thick AlN thin film.

curve,  $\text{NH}_3$  flow rate and duration were kept constant at 50 sccm and 20 seconds, respectively. Deposition rate increased with increasing TMA dose until 0.05 seconds, where growth rate saturated at  $\sim 0.76$  Å/cycle. For the  $\text{NH}_3$  saturation curve, TMA dose was kept constant at 0.05 seconds and  $\text{NH}_3$  flow duration was varied with

constant flow rate (i.e., 50 sccm). Deposition rate increased with increasing  $\text{NH}_3$  flow duration until maximum rate of  $\sim 0.86$  Å/cycle was obtained at 40 seconds. Increasing  $\text{NH}_3$  dose to 60 seconds did not increase the deposition rate. Deposition rates of AlN thin films at different temperatures are given in Figure 1(b). For these experiments, 100 cycle depositions were carried out with TMA and  $\text{NH}_3$  plasma pulse times of 0.1 and 40 seconds, respectively. Deposition rate remained constant at  $\sim 0.86$  Å/cycle for temperatures up to 200 °C, and then increased with increasing temperature. Temperature range, in which the deposition rate is constant, corresponds to the ALD window where surface reactions take place in a self-limiting manner. AlN growth rate increased with temperature starting from  $\sim 225$  °C. This result is consistent with the previous PEALD study reported by Liu et al.,<sup>14</sup> where no self-limiting growth behavior was observed for temperatures ranging from 250 to 470 °C. Film thickness versus number of deposition cycles is given in the inset of Figure 1(b). Film thickness increases linearly with increasing number of cycles, confirming that the deposition rate is constant at this temperature, i.e., 185 °C. Results also suggest that deposition starts immediately with the first cycle, without any incubation period. Figure 2 shows the cross-sectional SEM image of the  $\sim 100$  nm thick AlN

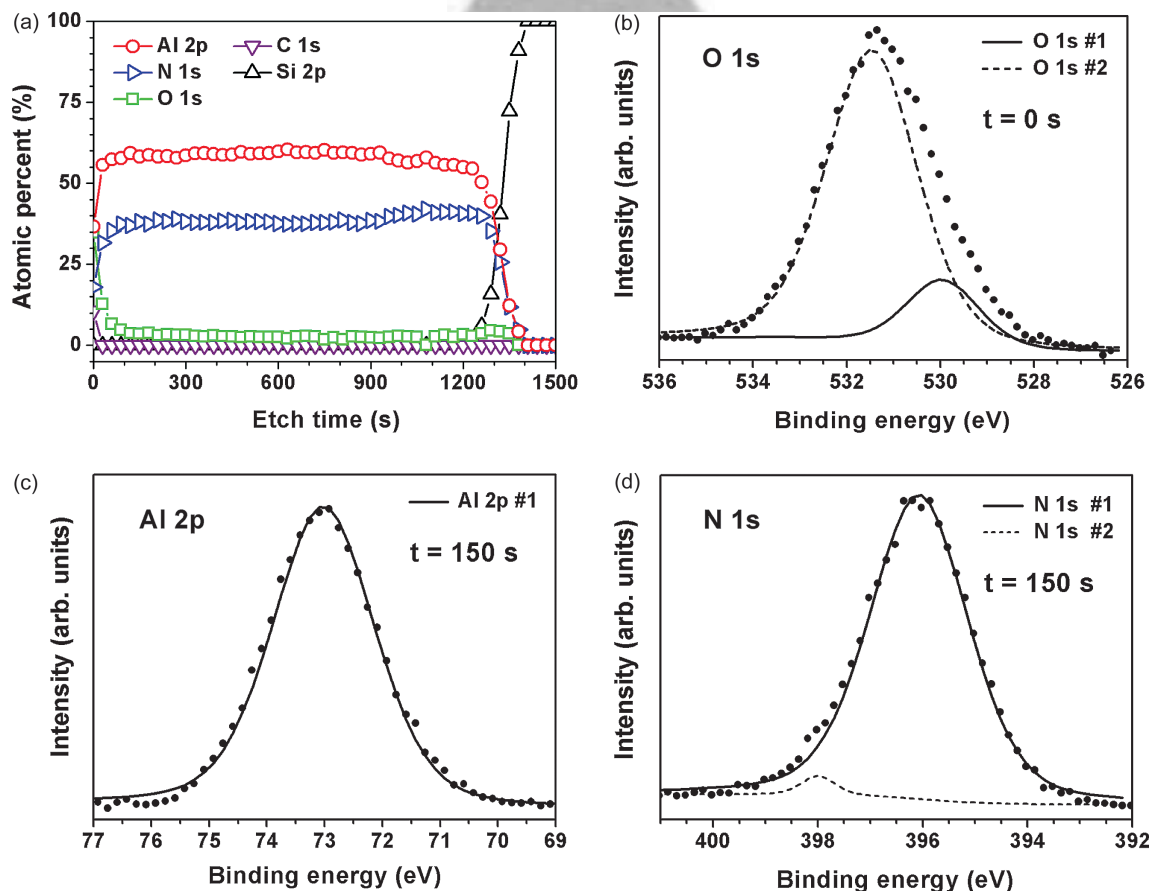
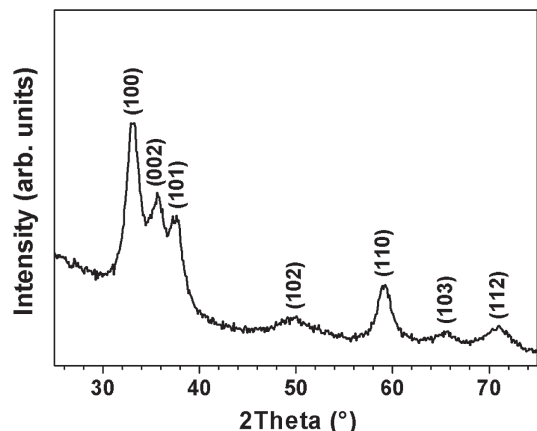


Fig. 3. (a) Compositional depth profile of  $\sim 100$  nm thick AlN thin film. (b) O 1s, (c) Al 2p, and (d) N 1s high resolution XPS scans.



**Fig. 4.** GIXRD pattern of  $\sim 100$  nm thick AlN thin film deposited on Si (100). Film is polycrystalline with a hexagonal wurtzite structure.

film deposited on Si(100) substrate, which confirmed the film thickness measurements performed by spectroscopic ellipsometry.

Compositional characterization of  $\sim 100$  nm thick AlN film deposited on Si(100) at  $185^\circ\text{C}$  was carried out by

using XPS. Survey scans detected peaks of aluminum, nitrogen, oxygen, and carbon. Figure 3(a) is the compositional depth profile showing that atomic concentrations of Al and N are constant in the bulk film. Although O concentration is high (35 at.%) at the film surface, it decays rapidly within the first 120 s. At 600 s, concentrations of Al, N, and O are 59.8, 37.6, and 2.6 at.%, respectively. Carbon is detected only at the film surface and there are no C impurities in the bulk film, indicating that efficient removal of methyl ( $\text{CH}_3$ ) groups from TMA was achieved by the use of  $\text{NH}_3$  plasma.

O 1s high resolution XPS scan given in Figure 3(b) represents the film surface, whereas Al 2p and N 1s scans given in Figures 3(c) and (d) refer to bulk film (etch time = 150 s). O 1s scan was fitted by two peaks located at 529.96 and 531.46 eV, corresponding to Al–O–N<sup>18</sup> and Al–O<sup>19</sup> bonds, respectively. Results, which indicate oxidation at the film surface, are similar to those reported in the literature for air-exposed AlN thin films deposited by plasma source MBE.<sup>19</sup> Al 2p data was fitted with a single peak at 73.02 eV (Fig. 3(c)), which is assigned to the

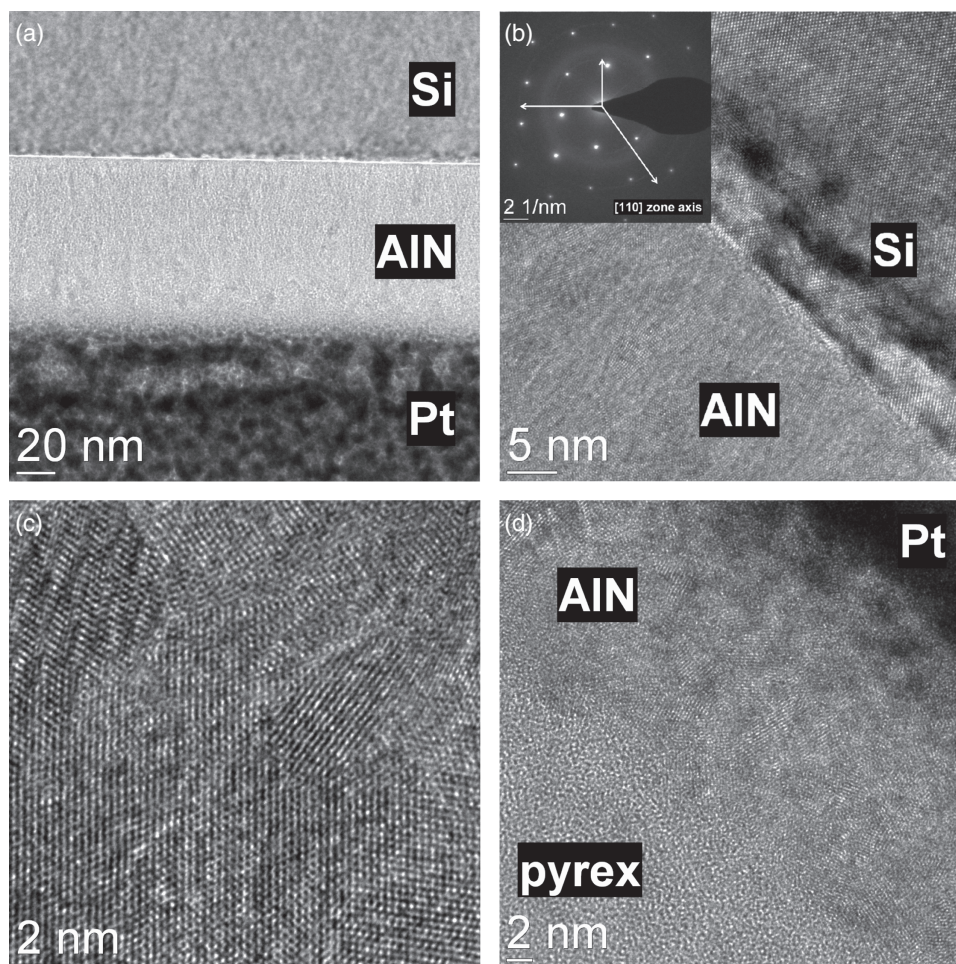


**Fig. 5.** (a) Cross-sectional TEM image of  $\sim 100$  nm thick AlN thin film deposited at  $185^\circ\text{C}$  on Si(100). (b, c) Cross-sectional HR-TEM images, and (inset) SAED pattern of the same sample. (d) Cross-sectional HR-TEM image of AlN thin film deposited on glass substrate.

Al–N bond.<sup>19,20</sup> Additional information about the chemical bonding states in the films is provided by the N 1s spectrum that was fitted by two peaks as shown in Figure 3(d). N 1s peak at 396.07 eV, which is assigned to the N–Al bond,<sup>21</sup> confirms the presence of AlN. Peak at 398.0 eV (N–Al–O bond<sup>30</sup>), on the other hand, corresponds to the <5 at.% O present in the bulk film.

AlN thin films deposited on Si(100) were polycrystalline as determined by GIXRD. Figure 4 shows the GIXRD pattern of ~100 nm thick AlN film, where (100), (002), (101), (102), (110), (103), and (112) reflections of the hexagonal wurtzite phase were observed. Similar patterns were obtained for the films deposited on Si(111), c-plane sapphire, MOCVD-grown GaN on c-plane sapphire, and glass substrates, with only difference being the more pronounced intensity of (100) reflection in the case of sapphire and GaN/sapphire substrates.

Figure 5(a) is the cross-sectional TEM image of the AlN film deposited on Si(100). Film thickness was measured as 95.9 nm from this image, which is in good agreement with the results obtained by ellipsometry. Figures 5(b) and (c) are the high-resolution TEM (HR-TEM) images of the same sample, showing a film microstructure consisting of nanometer sized crystallites. Selected area electron diffraction (SAED) pattern of this film is also given in the inset of Figure 5(b). In this pattern, reciprocal lattice points correspond to the diamond lattice of Si substrate. Diffraction rings, on the other hand, refer to AlN thin film and indicate a polycrystalline nature. HR-TEM image of the polycrystalline AlN thin film deposited on amorphous glass substrate is given in Figure 5(d), which again confirms the crystalline nature of the film independent of the substrate material.

### 3.2. PEALD of GaN

GaN thin films were deposited on Si(100) substrates by plasma-enhanced atomic layer deposition (PEALD) using trimethylgallium (TMG) and ammonia (NH<sub>3</sub>). TMG saturation behavior was studied at 185 °C with a constant NH<sub>3</sub> flow duration of 40 s. TMG doses of 0.015 and 0.03 s resulted with the same deposition rate (0.46 Å/cycle), indicating that saturation was already achieved at the minimum available TMG pulse time. This is due to the very high vapor pressure of TMG at room temperature. The excessive usage of TMG might be avoided by lowering the temperature of TMG until a decrease in deposition rate is observed. Figure 6 is the NH<sub>3</sub> saturation curve at 185 °C. Deposition rate increased with NH<sub>3</sub> flow duration until 90 s and reached saturation at ~0.56 Å/cycle. Inset of Figure 6 shows deposition rates of GaN thin films at different temperatures, where 100 cycles were deposited with 0.015 s TMG/10 s purge/90 s (50 sccm) NH<sub>3</sub>/10 s purge. A constant deposition rate of ~0.51 Å/cycle was observed within the temperature range of 250–350 °C. For temperatures in the range of 185–250 °C, deposition rate increased

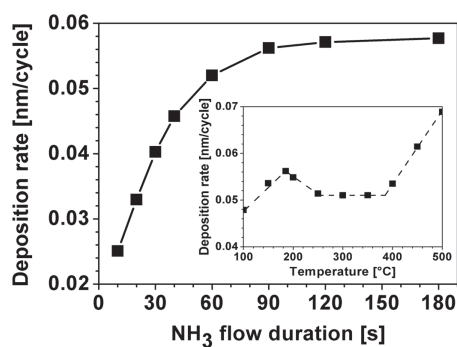


Fig. 6. NH<sub>3</sub> saturation curve for GaN at 185 °C. TMG dose was constant at 0.015 s. (Inset) Deposition rate of GaN as a function of temperature.

with decreasing temperature. This behavior is believed to be related to the purging efficiency, which decreases at lower temperatures.

Another set of GaN thin films were deposited on Si(111) substrates by PEALD using triethylgallium (TEG) and NH<sub>3</sub> as the Ga and N precursors, respectively. Figure 7(a) is the TEG saturation curve at 150 °C. Deposition rate increased with the TEG dose until 1 s. A further increase in TEG dose did not affect the deposition rate, implying that the chemisorption of TEG is self-limiting. Effect of purge time on deposition rate at 150 °C is given in the inset of Figure 7(a). Deposition rate decreased from 0.60

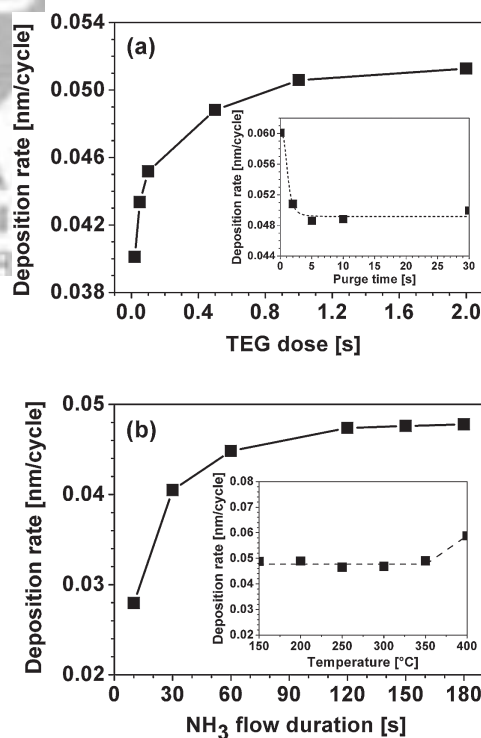


Fig. 7. (a) TEG saturation curve at 150 °C. NH<sub>3</sub> flow duration was constant at 90 s. (Inset) Deposition rate as a function of purge time. (b) NH<sub>3</sub> saturation curve at 250 °C. TEG dose was constant at 0.5 s. (Inset) Deposition rate of GaN as a function of temperature.

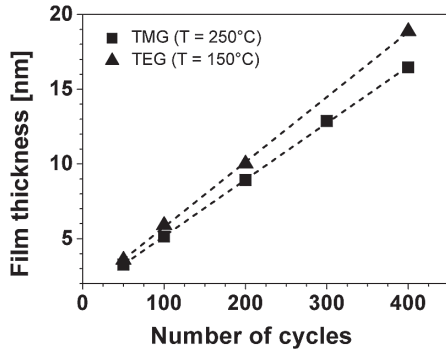


Fig. 8. GaN film thickness versus number of deposition cycles.

to  $0.49 \text{ \AA/cycle}$  as the purge time increased from 0 to 5 s, and remained constant at this value for longer purge times. Figure 7(b) shows the  $\text{NH}_3$  saturation curve at  $250^\circ\text{C}$ . Deposition rate increased with  $\text{NH}_3$  flow duration until 120 s and reached saturation at  $\sim 0.47 \text{ \AA/cycle}$ . Deposition rates of GaN thin films at different temperatures are given in the inset of Figure 7(b). For these experiments, 200 cycles were deposited with 0.5 s TEG/10 s purge/90 s (50 sccm)  $\text{NH}_3$ /10 s purge. A constant deposition rate of  $\sim 0.48 \text{ \AA/cycle}$  was observed within the temperature range of  $150\text{--}350^\circ\text{C}$ . For higher temperatures, deposition rate increased with temperature.

Film thickness versus number of deposition cycles graphs for GaN films deposited at  $250^\circ\text{C}$  using 0.015 s TMG with 90 s  $\text{NH}_3$ , and at  $150^\circ\text{C}$  using 1 s TEG with 120 s  $\text{NH}_3$  are given in Figure 8. A linear growth behavior was observed for both processes.

Compositional characterizations of the  $\sim 16$  and  $27 \text{ nm}$  thick GaN films deposited using TMG and TEG precursors, respectively, were carried out by using X-ray photoelectron spectroscopy (XPS). Survey scans detected peaks of gallium, nitrogen, oxygen, and carbon. Carbon was detected only at the film surfaces and no C impurities were found in the bulk films. Oxygen contents of the films deposited using TMG and TEG precursors were 19.5 and 22.5 at.%, respectively. Figure 9 represents

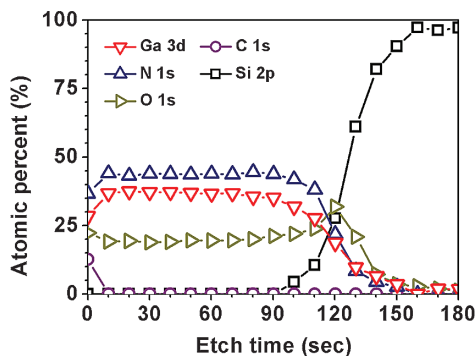


Fig. 9. XPS depth profile of  $\sim 16 \text{ nm}$  thick GaN thin film deposited at  $250^\circ\text{C}$  using TMG precursor.

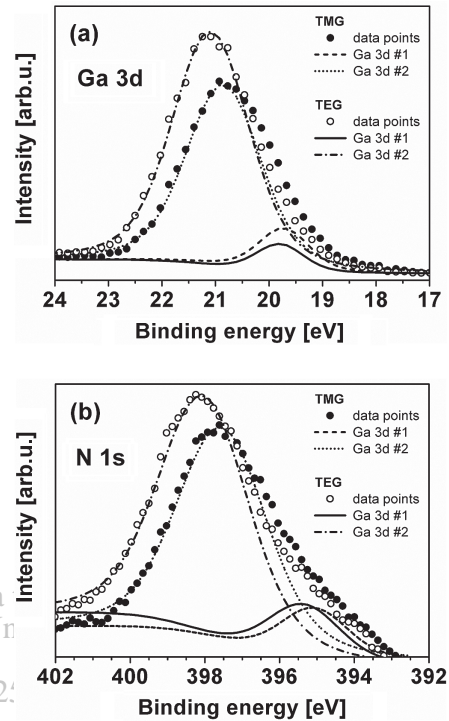


Fig. 10. (a) Ga 3d, and (b) N 1s high resolution XPS scans of GaN thin films.

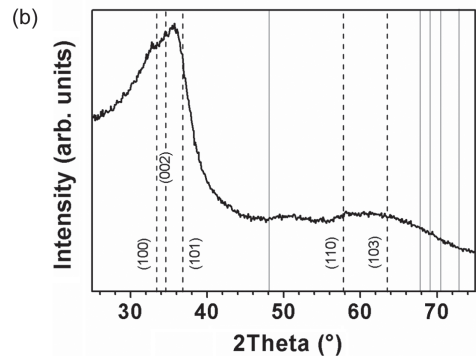
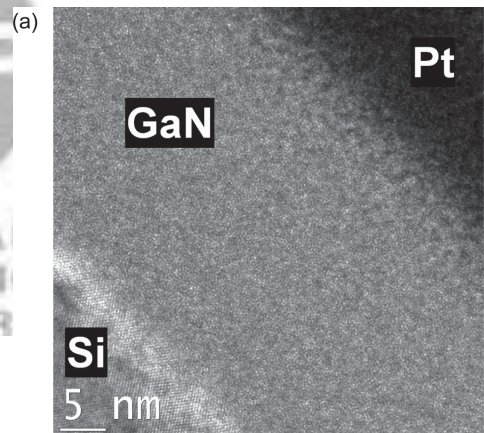


Fig. 11. (a) Cross-sectional HR-TEM images of GaN thin film deposited at  $250^\circ\text{C}$  on Si(100) substrate using TMG precursor. (b) GIXRD pattern of the same sample.

the compositional depth profile of the 16 nm-thick GaN deposited with TMG.

Ga 3d and N 1s high resolution XPS scans given in Figure 10 refer to bulk films. In Figure 10(a), Ga 3d scan of the film deposited using TMG was fitted by two peaks located at 19.72 and 20.85 eV, which correspond to Ga–N<sup>10,11</sup> and Ga–O<sup>22</sup> bonds, respectively. Similarly, two subpeaks located at 19.8 and 21.09 eV were assigned as Ga–N<sup>22,23</sup> and Ga–O<sup>22</sup> bonds, respectively, for the film deposited using TEG as the group-III precursor. In both cases, the intensity of Ga–O subpeak was higher than that of the Ga–N subpeak. N 1s scans of the films are given in Figure 10(b). Subpeaks located at 395.07 (TMG) and 395.35 eV (TEG) were assigned as the N–O bond,<sup>20,18</sup> whereas the ones located at 397.54 (TMG) and 398.03 eV (TEG) were assigned as the N–Ga.<sup>24,25</sup> Both Ga 3d and N 1s scans were shifted to higher energies when TEG was used as the group-III precursor.

High-resolution TEM (HR-TEM) image of GaN thin film deposited with TMG at 250 °C is given in Figure 11(a). Film was found to be composed of small, sub-nm crystallites dispersed in an amorphous matrix. GIXRD pattern of the same sample is also given in Figure 11(b), where hexagonal wurtzite structure is barely seen and dominant amorphous character is observed.

#### 4. CONCLUSION

In summary, we have deposited AlN and GaN thin films at temperatures as low as 100 °C with saturated deposition rates of ~0.86 Å/cycle and ~0.56 Å/cycle. Self-limiting growth behavior was observed for temperatures up to 200 °C and 350 °C for AlN and GaN films, respectively. For higher deposition temperatures, growth rate increased with substrate temperature. Within the ALD temperature windows (100–200 °C for AlN, 150–350 °C for GaN), film thicknesses increased linearly with the number of deposition cycles and no incubation behavior was observed. Self-limited grown AlN thin films were crystalline with a hexagonal wurtzite structure regardless of the substrate selection. However, GaN films exhibited amorphous-like structures due to the significantly high oxygen incorporation.

**Acknowledgments:** This work was performed at UNAM supported by the State Planning Organization (DPT) of Turkey through the National Nanotechnology

Research Center Project. GaN/sapphire templates were provided by U. Ozgur and H. Morkoc from Virginia Commonwealth University. Necmi Biyikli acknowledges support from Marie Curie International Re-integration Grant (Grant # PIRG05-GA-2009-249196).

#### References and Notes

1. S. C. Jain, M. Willander, J. Narayan, and R. Van Overstraeten, *J. Appl. Phys.* 87, 965 (2000).
2. H. Amano, N. Sawaki, I. Akasaki, and Y. Toyoda, *Appl. Phys. Lett.* 48, 353 (1986).
3. H. Lu, W. J. Schaff, J. Hwang, H. Wu, G. Koley, and L. F. Eastman, *Appl. Phys. Lett.* 79, 1489 (2001).
4. M. M. De Souza, S. Jejurikar, and K. P. Adhi, *Appl. Phys. Lett.* 92, 093509 (2008).
5. L. Shen, S. Heikman, B. Moran, R. Coffie, N.-Q. Zhang, D. Buttari, I.P. Smorchkova, S. Keller, S. P. DenBaars, and U. K. Mishra, *IEEE Electr. Device Lett.* 22, 457 (2001).
6. M.-A. Dubois and P. Mural, *Appl. Phys. Lett.* 74, 3032 (1999).
7. F. Serina, K. Y. S. Ng, C. Huang, G. W. Auner, L. Rimai, and R. Naik, *Appl. Phys. Lett.* 79, 3350 (2001).
8. Z. Chen, S. Newman, D. Brown, R. Chung, S. Keller, U. K. Mishra, S. P. DenBaars, and S. Nakamura, *Appl. Phys. Lett.* 93, 191906 (2008).
9. M. Leskela and M. Ritala, *Thin Solid Films* 409, 138 (2002).
10. R. L. Puurunen, *J. Appl. Phys.* 97, 121301 (2005).
11. Y. J. Lee and S.-W. Kang, *Thin Solid Films* 446, 227 (2004).
12. Y. J. Lee, *J. Cryst. Growth* 266, 568 (2004).
13. D. Riihela, M. Ritala, R. Matero, M. Leskela, J. Jokinen, and P. Haussalo, *Chem. Vap. Deposition* 2, 277 (1996).
14. X. Liu, S. Ramanathan, E. Lee, and T. E. Seidel, *Mat. Res. Soc. Symp. Proc.* 811, D1.9.1 (2004).
15. D. Eom, S. Y. No, C. S. Hwang, and H. J. Kim, *J. Electrochem. Soc.* 153, C229 (2006).
16. K.-H. Kim, N.-W. Kwak, and S. H. Lee, *Electron. Mater. Lett.* 5, 83 (2009).
17. O. H. Kim, D. Kim, and T. Anderson, *J. Vac. Sci. Technol. A* 27, 923 (2009).
18. C. C. Wang, M. C. Chiu, M. H. Shiao, and F. S. Shieu, *J. Electrochem. Soc.* 151, F252 (2004).
19. L. Rosenberger, R. Baird, E. McCullen, G. Auner, and G. Shreve, *Surf. Interface Anal.* 40, 1254 (2008).
20. D. Manova, V. Dimitrova, W. Fukarek, and D. Karpuzov, *Surf. Coat. Technol.* 106, 205 (1998).
21. H. M. Liao, R. N. S. Sodhi, and T. W. Coyle, *J. Vac. Sci. Technol. A* 11, 2681 (1993).
22. V. Matolin, S. Fabik, J. Glosik, L. Bideux, Y. Ould-Metidji, and B. Gruzza, *Vacuum* 76, 471 (2004).
23. P. Kumar, M. Kumar, Govind, B. R. Mehta, and S. M. Shivaprasad, *Appl. Surf. Sci.* 256, 517 (2009).
24. Z. Majlinger, A. Bozanic, M. Petravic, K.-J. Kim, B. Kim, and Y.-W. Yang, *Vacuum* 84, 41 (2010).
25. M. Drygas, R. T. Paine, and J. F. Janik, *Pol. J. Chem. Technol.* 8, 60 (2006).

Received: 10 October 2011. Accepted: 15 July 2012.